A Label-Free, Sensitive, Real-Time, Semiquantitative Electrochemical Measurement Method for DNA Polymerase Amplification (ePCR)

ARTICLE *in* ANALYTICAL CHEMISTRY · APRIL 2015

Impact Factor: 5.64 · DOI: 10.1021/acs.analchem.5b00079

7 AUTHORS, INCLUDING:

Nihan Aydemir

University of Auckland

12 PUBLICATIONS **35** CITATIONS

SEE PROFILE

Hazel Mcardle

Dublin City University

4 PUBLICATIONS **18** CITATIONS

SEE PROFILE

Jadranka Travas-Sejdic

University of Auckland

199 PUBLICATIONS **3,474** CITATIONS

SEE PROFILE

David E Williams

University of Auckland

338 PUBLICATIONS **7,489** CITATIONS

SEE PROFILE

analytical chemistry

Article

pubs.acs.org/ac

A Label-Free, Sensitive, Real-Time, Semiquantitative Electrochemical Measurement Method for DNA Polymerase Amplification (ePCR)

Nihan Aydemir,[†,‡] Hazel McArdle,[†,§] Selina Patel,[▽] Whitney Whitford,[▽] Clive W. Evans,[▽] Jadranka Travas-Sejdic,*[,†,‡] and David E. Williams*[,†,‡]

[†]MacDiarmid Institute for Advanced Materials and Nanotechnology, [‡]Polymer Electronics Research Centre, School of Chemical Sciences, University of Auckland, Private Bag 92019, Auckland 1022, New Zealand

[▽]School of Biological Sciences, University of Auckland, Auckland 1022, New Zealand

Supporting Information

ABSTRACT: Oligonucleotide hybridization to a complementary sequence that is covalently attached to an electrochemically active conducting polymer (ECP) coating the working electrode of an electrochemical cell causes an increase in reaction impedance for the ferro-ferricyanide redox couple. We demonstrate the use of this effect to measure, in real time, the progress of DNA polymerase chain reaction (PCR) amplification of a minor component of a DNA extract. The forward primer is attached to the ECP. The solution contains other PCR components and the redox couple. Each cycle of amplification gives an easily measurable impedance increase. Target concentration can be estimated by cycle count to reach a threshold impedance. As proof of principle, we demonstrate an electrochemical real-time quantitative PCR (e-PCR) measurement in the total DNA extracted from chicken blood of an 844 base pair region of the mitochondrial Cytochrome c oxidase gene, present at ∼1 ppm of total DNA. We show that the detection and semiquantitation of as few as 2 copies/μL of target can be achieved within less than 10 PCR cycles.

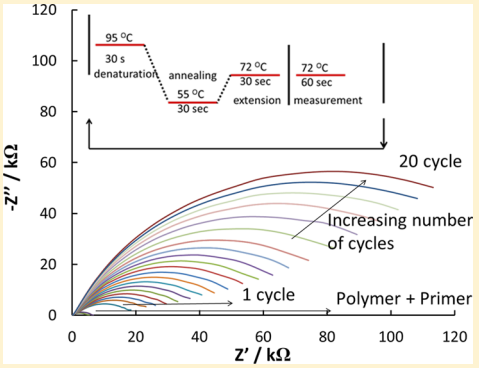

Amplification of nucleic acid sequences using the polymerase chain reaction (PCR) provides a powerful technology for both their detection and quantification.[1−5] Standard DNA PCR amplification is used primarily for the detection of particular sequences and is commonly assessed through the use of intercalation dyes, such as ethidium bromide, to detect the presence of specific products on electrophoretic gels. In quantitative PCR (qPCR), the amplification of specific sequences may be measured by using different intercalation dyes, such as SYBER Green, which fluoresce in the presence of double-stranded DNA. Alternatively, DNA amplification can be measured through the use of Taqman probes designed to bind to specific sequences between the amplifying primers.[6] As with intercalation dyes in qPCR, these probes also rely on the use of fluorescence methods for detection.[7] Electrochemical measurement in principle offers many advantages, in instrumentation, measurement system design, and cost of implementation, as exemplified by modern glucose measurement devices.[8] Hence, there has been significant interest in the electrochemical measurement of DNA[9−14] and several reports of coupling of electrochemical measurement with PCR or with various isothermal amplification methods.[15−17] These methods, again, have either used intercalation reagents for nonspecific measurement or electrochemical labels on the primers or nucleotides. The most sophisticated and now-commercialized methodology uses pH-sensitive field-effect transistors integrated into microwells[18] to detect the pH change caused by nucleotide incorporation.[19] The sensitivity (signal/noise or signal/background) of the measurement technique determines the number of cycles of amplification required to obtain a reliable signal, which, in turn, determines the time to result and also the influence of replication errors.

We and other researchers[11,20−28] have described oligonucleotide measurement based on the exclusion of a highly charged redox probe ($Fe(CN)_6^{3-/4-}$) from the electrode interface, as a result of the large negative surface charge introduced by the binding of oligonucleotides. Electrochemically active conducting polymers (ECP) can be used advantageously both as the active electrode and as the means of surface conjugation of a probe nucleotide.[29] The inhibition of the redox reaction of the polymer itself, through inhibition of the associated anion exchange with the solution, can also be used as the signal.[25−28] The presence in solution at concentrations in the low nanomolar (nM) to femtomolar (fM) range[13,20,22,30] or even lower concentrations[26] of purified nucleotide sequences that are complementary to a surface-attached probe can be measured relatively easily. The signal increases as the length of the target oligonucleotide sequence increases,[21] although with the caveat that the hybridization efficiency may decrease as the target length increases.[11,31] However, the measurement is based on

Received: January 7, 2015
Accepted: April 27, 2015

DOI: 10.1021/acs.analchem.5b00079
Anal. Chem. XXXX, XXX, XXX−XXX

the detection of global changes in the charge trapped at the reaction interface,[11,20,27] and so the measurement may be changed as a consequence of adsorption at the interface of any charged species, such as a protein or, indeed, from several other effects that alter the rate of reaction of the redox species. Thus, issues that are prominent include the need for calibration, repeatability of devices, nonspecific signals—effects of other species in the solution that may adsorb at the electrode surface and change surface charge and reaction rates as a consequence—and mismatched signals, where DNA that may not be completely complementary to the target can hybridize sufficiently with the surface-bound oligonucleotide to cause an alteration of the electrochemical reaction rate.

The combination of a high-sensitivity label-free electrochemical detection method with PCR (ePCR) offers specific attributes that overcome these problems, as well as the cost benefits generally associated with label-free electrochemistry. The particular advantage of PCR is that the composition of the solution steps in a defined way from one cycle to the next, the amplicon number ideally doubling. Therefore, any signal correlated precisely with each step in ePCR will be a signal that is derived specifically from the effect of the presence and amplification of the DNA target. The steps should be clear and distinct and progress in a well-defined way, and they should be clearly separable from any general, nonspecific drift in the electrochemical properties of the interface. A second feature of PCR is that it offers a digital encoding of target DNA concentration: the number of steps required to reach a threshold signal reflects the initial concentration of the target. The threshold can be chosen to be sufficiently large, with respect to any baseline drifts of the detector. Consequently, real-time ePCR should show correlated signal steps, which evolve with time and cycle number and are dependent only on the presence of the target. The number of steps to reach an appropriately chosen threshold should relate directly to the original target concentration. The very high sensitivity of a label-free electrochemical detector should allow specific detection and quantification of target DNA in a small number of cycles—that is, within a timeframe that could be significantly shorter than that required for detection and quantification using optical fluorescence methods. Whether the use of a redox probe, such as $Fe(CN)_6^{3-/4-}$, affects the efficiency of the polymerase enzyme is something that would have to be checked.

The electrochemical and mechanical stability of the electrochemical measurement interface upon cycling to the high temperatures necessary to implement PCR is clearly important. The stability of attachment of the primer to the surface could be an issue for methods using metal chelation,[25] or methods using thiolate adsorption to gold,[11] but should be less of an issue if the primer is conjugated to a polymer by a direct chemical bond.[20] However, for methods utilizing conducting polymers, irregular or otherwise large changes in adhesion of the polymer to the electrode substrate, or in polymer microstructure, or in the state of oxidation or doping of the polymer, would cause changes in electrochemical reaction rate at the polymer/solution interface that would militate against reliable and quantitative measurement. Temperature stability of the conducting polymer interface is not necessarily to be expected.[32] Previous studies have shown a time-varying collapse of microstructure in aqueous buffer that is dependent on the nature of the polymer, the nature of the dopant ions, and the solvent system used for synthesis, which also has a significant effect on the adhesion of the polymer to the electrode substrate.[24,33−35] These effects might be expected to become even more important with increasing temperature.

In the present work, we have explored the use of label-free electrochemistry using an electrode coated with an ECP, with a $Fe(CN)_6^{3-/4-}$ redox couple in solution as the detection methodology for real-time, quantitative PCR. We have chosen the surface-attached probe sequence to be one primer for the amplification, so extension of this surface-attached primer by the polymerase enzyme could occur.[36,37] We demonstrate that the ECP—in this case, electrochemically co-polymerized pyrrole and 3-pyrrolylacrylic acid, poly(Py-*co*-PAA)—is sufficiently temperature-stable, such that (i) the baseline does not significantly drift, (ii) the presence of $Fe(CN)_6^{3-/4-}$, although it does, to a degree, inhibit solution amplification, does not adversely affect the amplification measured electrochemically, and (iii) the sequence selectivity of a surface-bound primer is such that reliable detection and quantification of a specific sequence present in a minor amount in a mixed background of DNA can be obtained using either the surface-immobilized forward primer alone, or the surface forward primer with either the reverse primer alone in solution or with both forward and reverse primers in solution. We present a simple model, based on the "patch" model previously described,[20] that adequately describes the evolution of the electrochemical reaction impedance as the amplification proceeds.

EXPERIMENTAL SECTION

More detail is given in the Supporting Information (SI).

Electrode Preparation. A film nominally 6−12 nm thick of ECP, which is a co-polymer of pyrrole and pyrrolylacrylic acid, was electrochemically grown on a glassy carbon electrode (GCE, see the SI). Electrodes having films that were relatively uniform and adherent were selected based on impedance measurement (see the SI). Figure 1C shows a typical scanning electron microscopy (SEM) image of the resultant polymer layer. The ECP-coated GC showed polymer nodules with a size scale up to 200 nm scattered across a thin underlying layer, which had a discernible microstructure that was distinct from any structure of the underlying glassy carbon, which was itself very smooth (Figure 1B). The layer was probably significantly thicker than the nominal 6−12 nm, and thus was significantly porous.

Electrochemical Measurement and Impedance Data Extraction. A two-terminal electrochemical cell was assembled in a 100 μL Eppendorf tube, suitable for insertion into a PCR temperature cycler. The working electrode was the polymer-functionalized GC and the counter/reference electrode was a Pt wire. Since the solution contained the ferri-ferrocyanide redox couple, the Pt electrode (to a reasonable approximation dependent on the current flowing) would adopt the redox potential for this couple. The base electrolyte (40 μL) was the PCR buffer (20 mM Tris-HCl, pH 8.4, 50 mM KCl) containing 2.5 mM $MgCl_2$ and 5 mM of each of $Fe(CN)_6^{3-/4-}$. Electrodes were checked by cyclic voltammetry and impedance measurement at 72 °C before and after surface attachment of the primer. All electrochemical impedance measurements in this work were obtained at a cell potential difference of +0.23 V over a frequency range from 100 kHz to 1 Hz. Figure 1A shows the diminution in reversibility of the redox couple caused by the coating of the surface by the polymer. The electrochemical impedance (Figure 1D) was characteristic of a microscopically rough interface, namely, a semicircle with the center depressed

DOI: 10.1021/acs.analchem.5b00079
Anal. Chem. XXXX, XXX, XXX−XXX

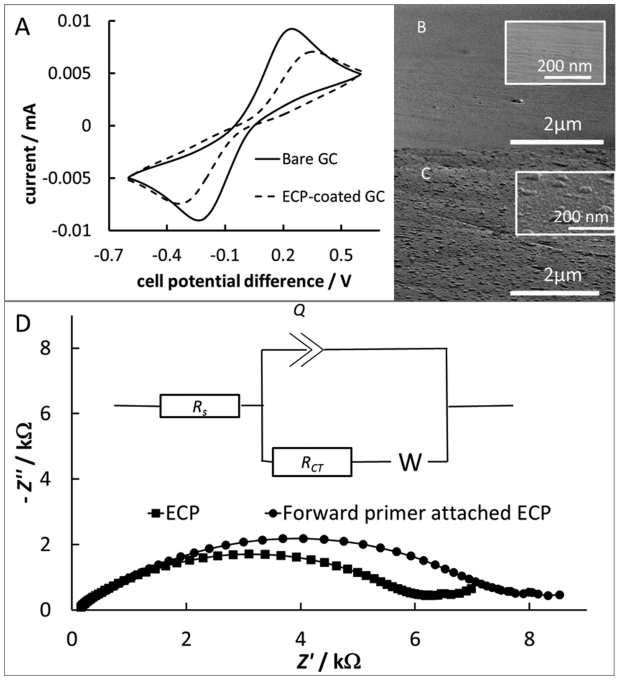

Figure 1. (A) Cyclic voltammetry (0.1 V/s) at 72 °C in the two-terminal electrochemical cell, of 5 mM $Fe(CN)_6^{3-/4-}$ in base electrolyte, comparing the bare glassy carbon electrode (GCE) with an electrode modified with a thin film of ECP. (B) SEM image of the bare GCE surface. (C) SEM of the ECP-coated GCE. (D) Electrochemical impedance (72 °C, +0.23 V cell potential difference) in base electrolyte containing 5 mM $Fe(CN)_6^{3-/4-}$, confirming successful attachment of the probe sequence from the resultant increase in impedance. The inset for panel D shows the approximate equivalent circuit: R_s, solution resistance between the working electrode and the counter/reference electrode; Q, constant phase element describing the capacitive behavior of the ECP-coated electrode; R_{CT}, charge transfer resistance for the reaction of the redox couple; and W, impedance contributed by diffusion of the redox couple to the electrode.

an angle $n\pi/2$ below the real impedance axis. The maximum value of the imaginary component of impedance, $(-Z'')_{max}$, for the approximate equivalent circuit over the frequency range where the diffusional impedance does not affect the data, is given as

$$(-Z'')_{max} = \frac{R_{CT}}{2}\left\{1 - \sin\left(\frac{n\pi}{2}\right)\right\} \quad (1)$$

Hence, provided n, which is dependent on the roughness of the interface,[38] does not greatly vary, $(-Z'')_{max}$, which we call the reaction impedance, is an easily obtained measure of the variation of the resistance due to the charge-transfer reaction of the redox couple (R_{CT}). We define the reaction conductance (σ) as

$$\sigma = \frac{1}{(-Z'')_{max}}$$

We have used this measure because it is pragmatic and practical, directly reflecting the raw experimental data; it is not dependent on arbitrary details of a specified equivalent circuit.

Materials. DNA was extracted from whole chicken blood by a standard proteinase K digestion and a modified version of the phenol/chloroform method.[39,40] Forward and reverse primers designed for amplification of a 844 base pair region of the mitochondrial Cytochrome c oxidase (CO1 or cox1) gene[39] were 26 bases long (see the SI). A thymidine 10-mer extension, amino-terminated, was used for covalent attachment of the forward primer to the ECP surface by standard EDC-NHS chemistry (see the SI). Successful primer attachment was verified by the increase in electrochemical impedance (Figure 1D).

PCR Protocol. The PCR solution, in addition to the base electrolyte, contained dNTPs (0.2 mM each), Taq polymerase (7×10^{-3} unit/μL), and the extracted DNA sample (1.2 ng/μL of chicken blood cell DNA for 1× dilution to 1.2 pg/μL for 1000× dilution). Solution primers were added at 0.5 μM. Experiments in the absence of Taq polymerase controlled for nonspecific impedance effects during cycling. The electrodes were open-circuit until the electrochemical impedance measurement was made, which, unless otherwise stated, was at 72 °C, following the extension time, and required 60 s to complete.

Quantification of the Target Concentration. Following solution amplification of the Cox1 template present in the chicken blood extract with the same forward and reverse primers used for ePCR, the amplified product was separated by gel electrophoresis, extracted, purified, and sequenced. The gel electrophoresis (Figure 2) confirmed clean amplification. The

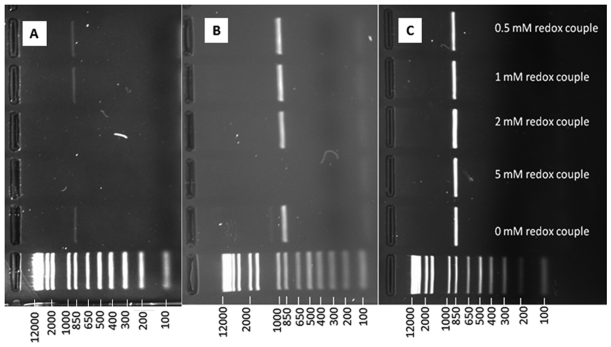

Figure 2. Gel electrophoresis of PCR solution amplification product (both forward and reverse primer present in solution) showing the effect of redox couple and Taq polymerase concentration. The first lane (lowest) is the scale in base pairs. Taq polymerase concentrations (unit/μL, cycle): (A) 7×10^{-3} unit/μL, 20 cycles; (B) 2.5×10^{-2} unit/μL, 25 cycles; and (C) 0.4 unit/μL, 25 cycles.

sequence of the amplified product was identical to part of a known chicken Cox1 DNA sequence (GenBank database AP003317.1). A standard curve was obtained using the purified, diluted product, and the mass of Cox1 template in the total chicken blood DNA extract was determined by standard q-PCR (details are given in the SI). The Cox1 template comprised 1 ppm of the total chicken blood DNA present. The 1× dilution of total DNA (1.2 ng/μL) contained 1.3 fg/μL or 1450 copies/μL of the Cox1 template.

RESULTS

Effect of the Redox Couple on Amplification of the Target Sequence. In the presence of the redox couple, the efficiency of the amplification in solution, as judged by gel electrophoresis (see Figure 2) decreased as the redox couple concentration increased, ameliorated by increases in enzyme concentration.

Temperature Stability of Electrochemical Behavior of ECP Electrodes. Temperature stability of the electrochemical impedance of the ECP-coated electrodes is critical to the

DOI: 10.1021/acs.analchem.5b00079
Anal. Chem. XXXX, XXX, XXX−XXX

reliability of the method. Initial explorations established that cyclic voltammetry on the ECP was reasonably stable at temperatures up to 95 °C, provided that the potential range was restricted to avoid irreversible oxidation or reduction of the polymer. The thermal stability of the ECP electrodes under the PCR measurement regime described above was then evaluated first by impedance measurement in the PCR/redox couple mixture in the absence of target DNA. This measurement also explores the stability of attachment of the primer to the electrode surface. The electrode impedance changed by <20% after 20 temperature cycles. In addition, cyclic voltammetry and impedance measurement of the electrode without attached primer in the absence of the redox couple, measured at 72 °C during the temperature cycling with the electrode otherwise at open circuit, showed a change of <20% in either the apparent capacitance of the electrode or the current due to the redox process of ion injection and removal.

Single-Primer PCR: Amplification from the Surface-Attached Forward Primer Alone. DNA polymerase is active on surface-bound templates.[36,37] In the absence of the reverse primer in the solution, the surface-bound primer would be extended to a length determined by the extension time. A statistical distribution of length of surface-bound single-stranded DNA is expected to result. Figure 3 illustrates that, with the surface-bound primer alone, in the presence of the chicken blood DNA containing the mitochondrial DNA target, 5 mM redox couple, and the low concentration of enzyme (Taq polymerase, 7×10^{-3} unit/μL), the impedance signal increased progressively with each temperature cycle. Figure 3A shows the evolution of the impedance diagram with cycle number (cycle 0 labels the impedance with the primer attached to the surface, measured in the absence of Taq polymerase). Figure 3B shows the evolution of the reaction impedance as defined in the Experimental Section ($(-Z'')_{max}$). Figure 3C shows the evolution of the relative change in reaction conductance after each cycle.

$$\frac{\Delta\sigma}{\sigma_0} = \frac{(-Z'')_{\text{max,cycle } n} - (-Z'')_{\text{max,cycle 0}}}{(-Z'')_{\text{max,cycle } n}} \quad (2)$$

The result is consistent with our previous observation that reaction impedance for the ferro-ferricyanide redox couple increases with increasing length of DNA coupled to the surface, and with our deduction that the mechanism is exclusion of the redox couple due to increase of surface charge on the electrode.[20,21] The result shows that there has been extension of the oligonucleotide on the surface, despite the initial studies in solution indicating a decrease in the efficiency of the amplification for this combination of redox couple and Taq polymerase concentration.

Electrochemical Measurement of PCR Amplification with Both Primers in Solution, Together with Surface-Bound Forward Primer. In this configuration (three-primer system), the target 844 bp sequence is amplified in solution as a double-stranded DNA, as expected in standard solution PCR. In addition, the surface-bound primer may also be extended, as in the case treated above. Following the dissociation step at 95 °C, during the annealing step at 55 °C, single-stranded DNA from the solution can be hybridized onto both the surface-bound extended primer and to any nonextended, surface-bound primer. Impedance diagrams had the same form as Figure 3. The reaction impedance evolved systematically with cycle number (see the SI) but was variable between repetitions. In

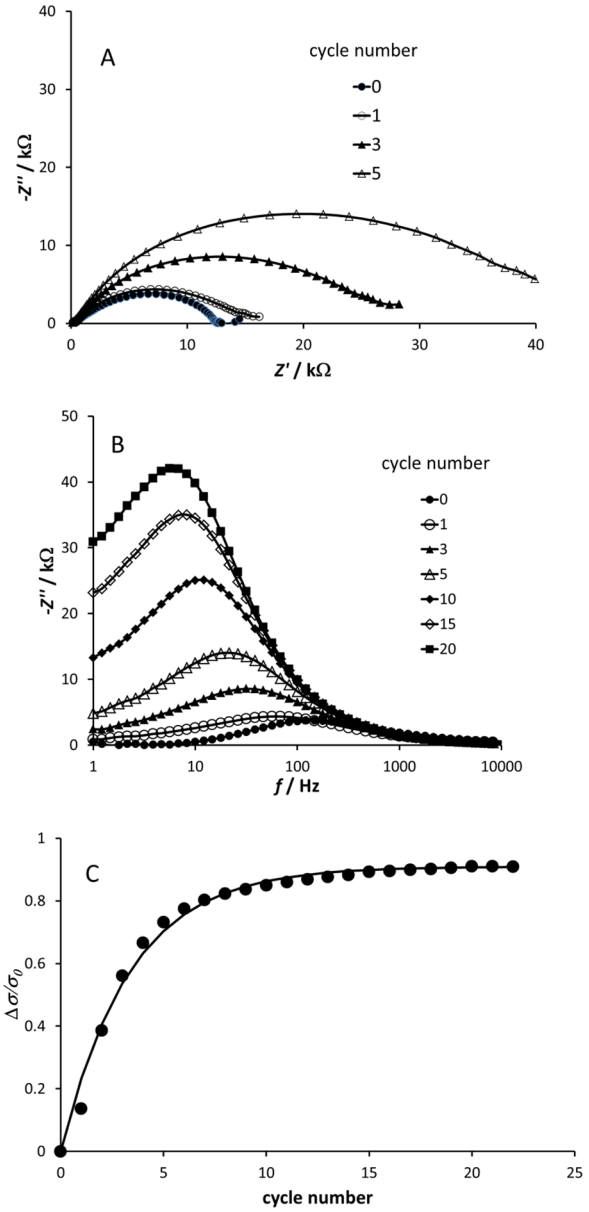

Figure 3. Amplification with surface-attached forward primer only. Measurements at 72 °C following extension, in the presence of 5 mM redox couple, +0.23 V cell pd (chicken blood DNA, 1.2 ng/μL, 7×10^{-3} unit/μL Taq): (A) evolution of impedance diagram with cycle number; (B) imaginary impedance component, $-Z''$, against measurement frequency, f and evolution with cycle number; and (C) evolution of relative reaction conductance (eq 2) with cycle number, where the line is fitted to a simple two-state model (see the Discussion section).

Figure 4A, the evolution, with cycle number, of the relative reaction conductance is shown. Figure 4A illustrates, by comparison with Figure 3C, that an additional amplification had indeed been obtained as a consequence of the presence of both primers in the solution, although, for this combination of redox couple and enzyme, concentration amplification in the solution had been inhibited, to some degree, by the presence of the redox couple (see Figure 2). Good reproducibility between different electrode preparations, and very high sensitivity for the method is demonstrated. Figure 4A shows a comparison of the signal (relative reaction conductance) evolution at 1000× dilution (1.2 pg/μL total DNA; 1.3 ag or ~2 copies/μL of the mitochondrial DNA target based on the quantification

DOI: 10.1021/acs.analchem.5b00079
Anal. Chem. XXXX, XXX, XXX−XXX

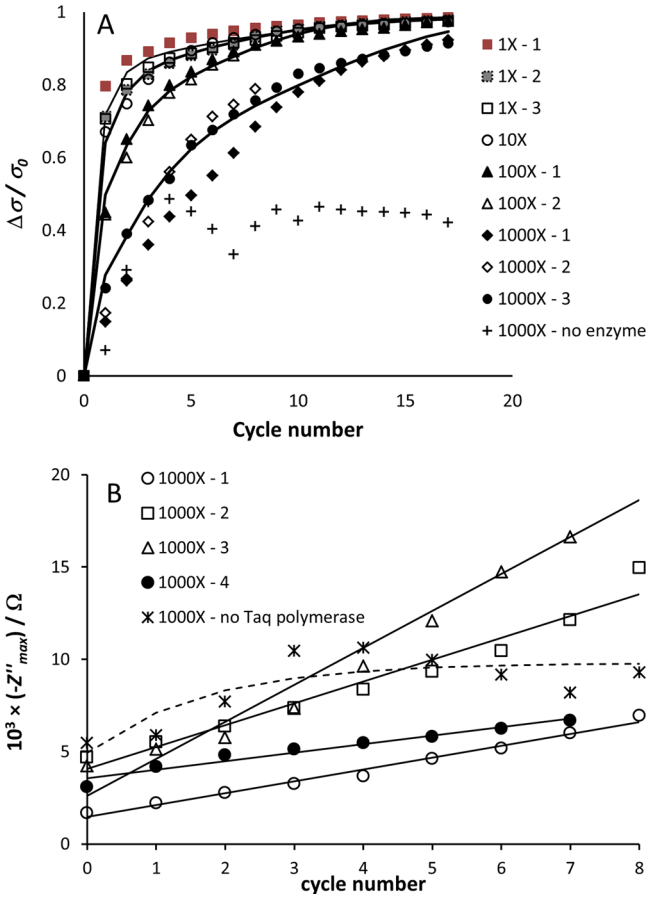

Figure 4. Evolution of (A) relative reaction conductance (eq 2) and (B) reaction impedance for the first cycles for the 1000× dilution including the initial measurement of the template-modified electrode and the Taq polymerase-free blank, for the three-primer system. Measurements at 72 °C following extension, 5 mM redox couple, and 7×10^{-3} unit/μL Taq polymerase at +0.23 V cell pd. The effect of dilution of the original chicken blood DNA sample is shown: from 1.2 ng/μL (1× dilution) to 1.2 pg/μL (1000× dilution). The lines in panel A are a fit to a four-state model (see the Discussion section) and those in panel B are empirical linear (Taq polymerase present) and exponential (Taq polymerase absent) fits. The repeat measurements shown are for independent electrode preparations.

described in the SI) in the presence and absence of the Taq polymerase. The signal for the Taq polymerase-free blank reached a plateau within the first three cycles. That, for the case with Taq polymerase present, exceeded the blank within <10 cycles and increased to the same level as that found for the higher concentrations of DNA target. Figure 4B shows the variation of the raw data (the reaction impedance) at 1000× dilution over the first few cycles, including the Taq polymerase-free blank (see the SI (Figure S4 shows the full dataset)). This illustrates the significant variation in reaction impedance for the primer-modified electrode (cycle 0: between 1−6 kΩ), which is the cause of the variability in evolution of reaction impedance. Figure 4B also shows the rapid approach to a plateau of reaction impedance in the absence of Taq polymerase, contrasting with the regular increase with cycle number in the presence of Taq polymerase. Detection of the presence of the target can be achieved just by observing the regular increase of reaction impedance with cycle number for a sufficient number of cycles to discriminate against any blank effects.

Quantification requires the use of the relative reaction conductance change and can be achieved by counting cycles to reach a threshold (see Figure 5). Such quantification requires the determination of the impedance of the primer-modified electrode before any amplification: $(-Z'')_{\max,\text{cycle }0}$ in eq 2.

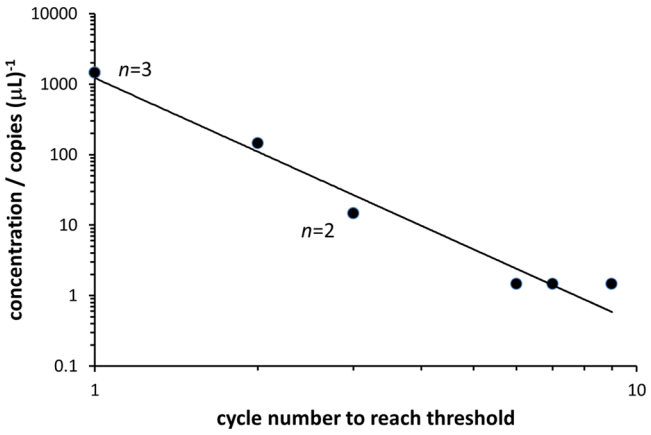

Figure 5. Cycle number to reach $\Delta\sigma/\sigma_0 > 0.7$, vs concentration of target in the diluted chicken blood DNA. Three-primer system: both primers in solution and forward primer on electrode. Repeat measurements on independent electrodes at dilutions from 1× to 1000× of 1.2 ng/μL total DNA shown; where these overlap, the number of independent determinations is shown.

Electrochemical Measurement of PCR Amplification with Reverse Primer Only in Solution, Together with Surface-Bound Forward Primer. In this configuration, the surface-bound primer may be extended, as described above. However, in the solution, single-stranded DNA will be formed by reaction from the single primer present, to a length defined by the extension time. This single-stranded DNA can be captured onto the surface-bound oligonucleotide (i.e., extended or nonextended primer) during the annealing step at 55 °C. Impedance diagrams had the same form as illustrated in Figure 3, and reaction impedance evolved with cycle number in a similar way to that shown in Figures 3 and 4. However, the results were not as reproducible.

Effects of Changing Measurement Temperature and Time Delay before Measurement. It is to be expected that the measurement signal would be altered as a consequence of the effects of the kinetics of the polymerase reaction both in the solution and on the electrode surface, as well as the effects of the diffusion of single-stranded DNA to the electrode surface, the kinetics of hybridization to the surface-bound oligonucleotide, and the competition for dissociated single-stranded DNA between solution hybridization and surface hybridization. The measurement could also just as conveniently be made at the end of the annealing step at 55 °C as at the end of the extension step at 72 °C. Figure 6 shows the effect of changing the annealing time, with measurements made for three successive temperature cycles between 95 °C and 55 °C. In this experiment, Taq polymerase was absent; the forward primer was present on the electrode surface. In the presence of the mixed DNA, the temperature was increased stepwise to 95 °C to dissociate surface-hybridized DNA. The temperature then was stepped back to 55 °C and successive impedance measurements were made at that temperature as the annealing proceeded. Figure 6 shows that the relative reaction conductance change approached a limit with a time constant

DOI: 10.1021/acs.analchem.5b00079
Anal. Chem. XXXX, XXX, XXX−XXX

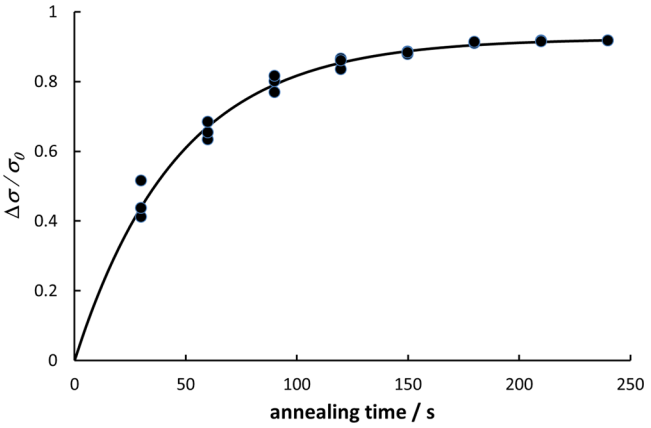

Figure 6. Relative reaction conductance change (eq 2) at 55 °C versus annealing time, following a step from 95 °C. Impedance measured in the absence of Taq polymerase. Total chicken blood DNA concentration = 1.2 ng/μL. The line is the fit to a simple exponential approach to a limit (see the Discussion section). Reaction conductance (σ_0) of the forward primer-modified electrode measured in the absence of DNA, 1600 Ω; projected reaction conductance from fit: 1100 Ω.

of ~84 s. Similarly, an increase in the extension time at 72 °C in the presence of the Taq polymerase gave an increase of reaction impedance. The choice of extension and annealing time represents a compromise between signal development at each cycle, stability of the electrochemical impedance during the time that the measurement is made, and the number of cycles that can be completed within a given analysis time. The reaction conductance (σ_0) of the forward-primer-modified electrode measured in the absence of DNA could be obtained by fitting the annealing time dependence of the relative reaction conductance to a simple exponential evolution with time, although not with great accuracy, given the time resolution of the measurements in the present work.

DISCUSSION

The hypothesis formulated earlier in this paper, that a label-free electrochemical method utilizing exclusion of a redox couple from the surface of an electrochemically active conducting polymer could be used as a high-sensitivity real-time measurement of the progress of PCR amplification of a minor component from total cellular DNA, has been demonstrated to be correct. Figure 5 illustrates that quantitation can be achieved by counting cycles to reach a threshold, and that the method has extremely high sensitivity that is obtainable within a small number of PCR cycles. The time scale for quantification at the highest dilution, with a target concentration in the ~2 copies/μL or ag/μL range was 25 min (7 cycles). A significant part of these times was that for temperature stabilization, which can be mitigated by appropriate design of the cell and cycler, and for measurement of the full impedance spectrum, which is clearly unnecessary. Figure 4 illustrates that the blank signal, in the absence of Taq polymerase, increased over the first two or three cycles and then stabilized. Although there may be some nonspecific binding of nontarget DNA (likely to occur in most complex PCR amplifications), the primer design and tuning of PCR conditions should minimize any such effect. Then, we can interpret the signal in the absence of Taq polymerase as being indeed due to binding of the target, the extent of which would depend on the concentration of target in the boundary layer near the electrode and increase over the first few cycles, as a consequence of dissociation from the surface of previously bound DNA, during the 95 °C part of the cycle.

Despite pre-existing caveats concerning the stability of the ECP, the present work has shown an adequate temperature stability in aqueous buffer for the system employed here. We presume that there were three factors that were important: (i) the conducting polymer layer was very thin; (ii) the synthesis used a solvent that was predominantly water, with just a small addition of organic solvent; and (iii) the ions doped into the polymer during synthesis were the same as those predominantly present in the measurement solution. In the following, we discuss the results using the simple patch model for the electrochemical kinetics previously presented:[20] the total current through the interface is the sum of that through different patches carrying different surface charge.

Figure 6 illustrates the simplest case: the annealing of the target sequence onto the surface primer, which is the first step of the first cycle. In this case, the surface-bound primer captures onto the interface the entire single DNA strand within which the complementary sequence is embedded. A two-patch model applies, with one patch being the hybridized fraction of the surface and the other being the unhybridized fraction. The conductance (σ) that is due to the interface reaction is the sum of the conductance through the unhybridized patches (σ_0) and that through the hybridized patches (σ_1):

$$\sigma = \theta_0\sigma_0 + (1 - \theta_0)\sigma_1 \tag{3}$$

where θ_0 denotes the fraction of the surface that is not hybridized. The variation with time t of the relative change in reaction conductance during the annealing step, where the reaction conductance for the state with unhybridized surface-attached primer only is σ_0, shows the progressive coverage of the surface by hybridized DNA. Figure 6 indicates that, in accord with our previous work,[20] this is a simple first-order kinetic process with a time constant τ:

$$\frac{\Delta\sigma}{\sigma_0} = (1 - \theta_0)\left[1 - \left(\frac{\sigma_1}{\sigma_0}\right)\right] = \left(1 - \frac{\sigma_1}{\sigma_0}\right)\left[1 - \exp\left(-\frac{t}{\tau}\right)\right] \tag{4}$$

The significance is that extrapolation back to the reaction impedance at t = 0 during annealing at 55 °C, following the initialization of the sequence at 95 °C, would give σ_0, the reaction conductance for the state with unhybridized surface-attached primer only, obviating the need for prior measurement of this number, which varies from one electrode to another (Figure 4B) but is also key to reducing the data onto the repeatable curve of relative reaction conductance against cycle number (Figure 4A). A better time resolution of the impedance changes than has been obtained in the present work would be needed for an accurate determination (see Figure 6).

The simplest measurement system of those studied here is that where the only primer present is that bound to the surface: the results are shown in Figure 3. We interpret the increase in reaction impedance (decrease in reaction conductance) on each cycle, shown in Figure 3, as being due to the progressive extension of surface-bound primer.[36] After dissociation then annealing, complementary single-strand DNA from the solution is annealed to the surface-bound primer. In the extension step, the hybridized, surface-bound primer is extended to an extent that is dependent on the extension time and the length of the hybridized complementary sequence, which is limited only by

DOI: 10.1021/acs.analchem.5b00079
Anal. Chem. XXXX, XXX, XXX−XXX

the length of the original DNA, since there is no second primer present in the solution. The cycle then repeats, upon which complementary DNA can be captured both onto the extended and unextended surface-bound primers. The theoretical curve for the evolution of relative reaction conductance with cycle number, shown in Figure 3C, was derived by approximating the heterogeneous collection of extended primer and extended, hybridized primer states as a single low-conductance state. The model is thus a simple two-state model. The progression from state 0 (unreacted primer) to state 1 (reacted primer) is presumed to occur via a simple first-order process during both annealing and extension. To simplify further, just one of these steps is assumed to be rate-limiting and, in view of the result shown in Figure 6, we assume that this is the annealing step. Thus, following step n, where t denotes the annealing time for each step,

$$\theta_{1,n} = \theta_{0,n-1} \exp\left(-\frac{t}{\tau}\right) \tag{5}$$

The reaction conductance at each step is the sum of that due to state 1 and that due to state 0 (see eq 3). The data can then be fitted with the two parameters t/τ and σ_1/σ_0, as shown in Figure 3C. For both the data in Figure 3 and the data in Figure 6, $\sigma_1/\sigma_0 \approx 0.09$. The redox couple is relatively strongly excluded from the interface, as a consequence of the surface charge due to the surface-bound primer and DNA. This effect might explain why the electrochemical surface extension proceeded satisfactorily, despite the effect of the redox couple on the solution extension (recall Figure 2).

In the three-primer system (results shown in Figures 4 and 5), amplification should occur in the solution, as well as extension on the surface. In the solution, the system would evolve rapidly to a multiplication of the fixed-length target DNA segment, whose concentration increases in each cycle: $c_{\text{target},n} = \alpha^n c_{\text{target},0}$, where the multiplication factor, $\alpha \approx 2$, is expected for the ideal case. Amplification of the target DNA sequence in the solution should lead to an increase of sensitivity above that obtained when the only effect is extension of the primer on the surface: indeed, this effect was observed. In this case, to take into account both the effect of extension of the primer on the surface and the effect of capture onto the surface of amplicons from the solution, the surface can be represented by a four-state model, as indicated in Figure 7: state 0 is the unextended, unhybridized surface-attached primer; state 1 is extended, unhybridized surface-attached primer; state 2 is unextended surface-attached primer hybridized to complementary target from the solution; and state 3 is extended, surface-attached primer hybridized to complementary target from the solution. Following an amplification cycle, after the denaturation step at 95 °C, only states 0 and 1 are present on the surface; states 2 and 3 are formed at 55 °C by annealing from the solution remaining from the previous extension step. In the subsequent extension step at 72 °C, conversion of state 2 to state 3 by the Taq polymerase occurs, as well as multiplication in the solution.

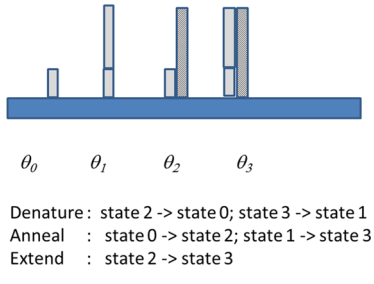

Figure 7. Schematic representation of the states for the surface-bound DNA, and the transitions during the PCR cycle; θ_j denotes the fraction of the surface covered by state j.

To take account of the effect of increase of solution amplicon concentration with cycle number, we assume that, during the annealing and extension phases, for the states $j = 0, 1$ where target DNA is captured onto the surface from the solution:

$$\left(\frac{d\theta_j}{dt}\right)_{\text{cycle } n} \approx -\frac{\alpha^n c_{\text{target},0}}{\tau} = -\frac{\alpha^n}{\tau'} \tag{6}$$

with time constant τ', which is independent of cycle number. For each cycle, the system is reset to a condition with no captured DNA—i.e., just states 0 and 1—at the end of the denaturing phase at 95 °C. Hence, using the subscript "d" to denote the relative surface coverages of states $j = 0$ at the end of the denaturing phase, in view of eq 6, we write

$$(\theta_{0,\text{d}})_{\text{cycle } n} = (\theta_{0,\text{d}})_{\text{cycle } n-1} \exp\left(-\frac{\alpha^{n-1}}{\tau'}\right) \tag{7}$$

$$(\theta_{1,\text{d}})_{\text{cycle } n} = 1 - (\theta_{0,\text{d}})_{\text{cycle } n} \tag{8}$$

Then, using the subscript "e" to denote the state of the system at the end of the extension phase at 72 °C, for states $j = 0, 1$:

$$(\theta_{j,\text{e}})_{\text{cycle } n} = (\theta_{j,\text{d}})_{\text{cycle } n} \exp\left(-\frac{\alpha^n}{\tau'}\right) \tag{9}$$

The relative coverage of the other states, $j = 2, 3$, is then easily obtained, because they are derived by conversion of states 0 and 1 during annealing and extension:

$$(\theta_{2,\text{e}})_{\text{cycle } n} = (\theta_{0,\text{d}})_{\text{cycle } n} - (\theta_{0,\text{e}})_{\text{cycle } n} \tag{10}$$

$$(\theta_{3,\text{e}})_{\text{cycle } n} = (\theta_{1,\text{d}})_{\text{cycle } n} - (\theta_{1,\text{e}})_{\text{cycle } n} \tag{11}$$

The reaction conductance is expressed as the sum of that from each of the individual states. Figure 4B shows the result of a least-squares fit to the experimental data of the relative reaction conductance thus predicted. The derived parameters are given in Table 1. Figure 8 shows the derived variation of the relative coverage of the four different states as the PCR cycling proceeds, for a sample where the total chicken blood DNA was diluted 1000×. Although the model is clearly oversimplified (e.g., τ' does not increase as expected with decreasing target concentration), the derived parameters allow some discussion of features of the results. First, the multiplication factor α is significantly less than 2, which is consistent with the effect of the redox couple on the solution amplification. This effect

Table 1. Fitting Parameters for Simple Four-State Model for the System with Both Primers in Solution and Forward Primer Surface-Attached

relative concentration	τ' /cycle	α	state	relative conductance
1	0.75	1.08	0	1
0.1	0.93	1.1	1	0.6
0.01	1.4	1.15	2	0.6
0.001	2.9	1.14	3	0.02

DOI: 10.1021/acs.analchem.5b00079
Anal. Chem. XXXX, XXX, XXX−XXX

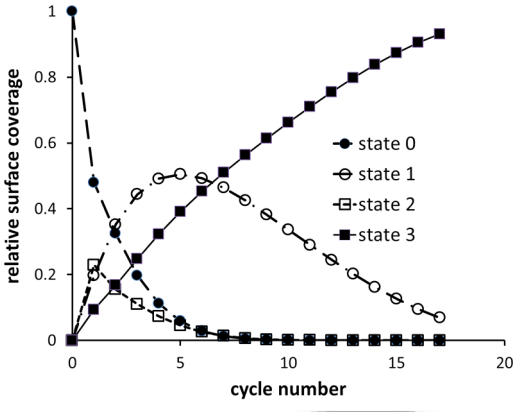

Figure 8. Evolution of relative surface coverages for the simple four-state model at a dilution of 1000× of total chicken blood DNA (data taken from Figure 4).

could be mitigated, as implied by Figure 2, by either increasing the concentration of the Taq polymerase or decreasing the concentration of the redox couple. However, such alterations involve compromises of cost (of Taq polymerase) and signal/noise (in the impedance measurement). Second, the signal development is dominated in the early cycles by the effect of extension of the surface primer and then in the later stages of the amplification by the capture of amplicons from solution. This is reasonable and accounts for much of the difference between the results of Figures 3 and 4. Third, the relative conductances due to states 1 and 2 are much greater than those suggested by the fitting of the two-state model to the data of Figures 3 and 6. This reflects both deficiencies of the model and subtleties in the evolution of the system that differs according to whether primers are present in the solution or not. In theory, the length to which the polymerase can extend the surface-attached primer is determined by the accessible length of the complementary strand hybridized to it. With no solution primers, this can proceed, in principle, to as much as the total length of the DNA sequence within which the target is embedded. However, with both primers present in solution, the target sequence itself will become the dominant complementary strand after a few cycles, resulting in the surface primer being extended only to the length of the target.

The discussion highlights that the high-temperature stage, at 95 °C, dissociates the untethered complementary DNA strand from the surface (i.e., the surface is "reset"). Thus, immediately after this step, the surface is in a defined reset condition of unhybridized primer, both extended and unextended, in proportion depending on the number of prior amplification cycles. Although we have not explored the possibility other than the results shown in Figure 6, clearly evolution of the signal from this "reset" state, and a systematic change from one cycle to the next, should provide another specific indicator of the presence of the target DNA.

CONCLUSION

Label-free, highly sensitive, real-time electrochemical detection of polymerase chain reaction amplification (ePCR) can be accomplished simply, using an electrochemically active conducting polymer as the electrode with one primer surface-bound, and the highly negatively charged redox couple $Fe(CN)_6^{3-/4-}$ in the solution as the signal species. Electrostatic exclusion of the redox couple from the electrode surface as the surface charge increases in each successive step of the PCR causes a successively stepping increase in the reaction impedance signaling the target-specific extension of surface-attached primers and amplification in the solution. We have shown, in proof of principle, that the ePCR method works successfully, despite some inhibition of the solution amplification by the redox couple. Once the detection system is in place, the technique is simple, rapid, and straightforward to apply. It needs only the addition of a redox couple to the standard PCR mix, and it does not require any fluorophores such as a Cy dye or a Taqman probe. It can be used both as a straightforward detection system and as a qPCR system, and has potential application wherever nucleic acid detection or quantitation is required.

ASSOCIATED CONTENT

Supporting Information

Materials, electrode preparation, electrode selection criteria, forward primer attachment procedure, measurement setup, ePCR protocol, complete data of reaction impedance evolution with cycle number for a three-primer system, quantitative PCR (qPCR) procedures, and results. The Supporting Information is available free of charge on the ACS Publications website at DOI: 10.1021/acs.analchem.5b00079.

AUTHOR INFORMATION

Corresponding Authors

*E-mail: j.travas-sejdic@auckland.ac.nz (J. Travas-Sejdic).
*E-mail: david.williams@auckland.ac.nz (D. E. Williams).

Present Address

[§]Dept. of Chemical Sciences, Dublin City University, Glasnevin, Dublin, 9, Ireland.

Author Contributions

All authors contributed to this manuscript and have given approval to its final version.

Notes

The authors declare no competing financial interest.

ACKNOWLEDGMENTS

This work was funded by the Tertiary Education Commission, New Zealand through the MacDiarmid Institute, by the NZ Ministry of Business, Innovation and Employment, through Contract No. C08X0806 (scholarship to N.A.), and by a Science Foundation Ireland Travel Scholarship to H.McA. (under Grant No. 10/IN.1/B3021).

REFERENCES

(1) Schmittgen, T. D.; Livak, K. J. *Nat. Protocols* **2008**, *3*, 1101−1108.
(2) Heid, C. A.; Stevens, J.; Livak, K. J.; Williams, P. M. *Genome Res.* **1996**, *6*, 986−994.
(3) Fraga, D.; Meulia, T.; Fenster, S. In *Current Protocols Essential Laboratory Techniques*; John Wiley & Sons: Hoboken, NJ, 2008.
(4) Bustin, S. A.; Mueller, R. *Clin. Sci.* **2005**, *109*, 365−379.
(5) Bartlett, J. M. S.; Stirling, D. In *PCR Protocols*; Bartlett, J. S., Stirling, D., Eds.; Humana Press: Totowa, NJ, 2003; pp 3−6.
(6) Van Guilder, H. D.; Vrana, K. E.; Freeman, W. M. *BioTechniques* **2008**, *44*, 619−626.
(7) Cao, H.; Shockey, J. M. *J. Agric. Food Chem.* **2012**, *60*, 12296−12303.
(8) Gubala, V.; Harris, L. F.; Ricco, A. J.; Tan, M. X.; Williams, D. E. *Anal. Chem.* **2012**, *84*, 487−515.
(9) Palecek, E.; Bartosik, M. *Chem. Rev.* **2012**, *112*, 3427−3481.

DOI: 10.1021/acs.analchem.5b00079
Anal. Chem. XXXX, XXX, XXX−XXX

(10) Kukol, A.; Li, P.; Estrela, P.; Ko-Ferrigno, P.; Migliorato, P. *Anal. Biochem.* **2008**, *374*, 143−153.
(11) Riedel, M.; Kartchemnik, J.; Schoning, M. J.; Lisdat, F. *Anal. Chem.* **2014**, *86*, 7867−7874.
(12) Travas-Sejdic, J.; Aydemir, N.; Kannan, B.; Williams, D. E.; Malmstrom, J. *J. Mater. Chem. B* **2014**, *2*, 4593−4609.
(13) Lazerges, M.; Bedioui, F. *Anal. Bioanal. Chem.* **2013**, *405*, 3705−3714.
(14) Dulgerbaki, C.; Oksuz, A. U.; Ahmad, S. *Electrochim. Acta* **2014**, *122*, 87−92.
(15) Lee, D. C.; Yip, S. P.; Lee, T. M. H. *Electroanalysis* **2013**, *25*, 1310−1315.
(16) Lusi, E. A.; Passamano, M.; Guarascio, P.; Scarpa, A.; Schiavo, L. *Anal. Chem.* **2009**, *81*, 2819−2822.
(17) Ren, Y.; Deng, H.; Shen, W.; Gao, Z. *Anal. Chem.* **2013**, *85*, 4784−4789.
(18) Toumazou, C.; Shepherd, L. M.; Reed, S. C.; Chen, G. I.; Patel, A.; Garner, D. M.; Wang, C.-J. A.; Ou, C.-P.; Amin-Desai, K.; Athanasiou, P.; Bai, H.; Brizido, I. M. Q.; Caldwell, B.; Coomber-Alford, D.; Georgiou, P.; Jordan, K. S.; Joyce, J. C.; La Mura, M.; Morley, D.; Sathyavruthan, S.; Temelso, S.; Thomas, R. E.; Zhang, L. *Nat. Methods* **2013**, *10*, 641−646.
(19) Zhang, F.; Wu, J.; Wang, R.; Wang, L.; Ying, Y. *Chem. Commun.* **2014**, *50*, 8416−8419.
(20) Kannan, B.; Williams, D. E.; Booth, M. A.; Travas-Sejdic, J. *Anal. Chem.* **2011**, *83*, 3415−3421.
(21) Booth, M. A.; Harbison, S.; Travas-Sejdic, J. *Biosens. Bioelectron.* **2011**, *28*, 362−367.
(22) Kannan, B.; Williams, D. E.; Laslau, C.; Travas-Sejdic, J. *Biosens. Bioelectron.* **2012**, *35*, 258−264.
(23) Peng, H.; Soeller, C.; Travas-Sejdic, J. *Macromolecules* **2007**, *40*, 909−914.
(24) Spires, J. B.; Peng, H.; Williams, D.; Travas-Sejdic, J. *Electrochim. Acta* **2011**, *58*, 134−141.
(25) Thompson, L. A.; Kowalik, J.; Josowicz, M.; Janata, J. *J. Am. Chem. Soc.* **2003**, *125*, 324−325.
(26) dos Santos Riccardi, C.; Kranz, C.; Kowalik, J.; Yamanaka, H.; Mizaikoff, B.; Josowicz, M. *Anal. Chem.* **2008**, *80*, 237−245.
(27) Kalantari, R.; Cantor, R.; Chen, H.; Yu, G.; Janata, J.; Josowicz, M. *Anal. Chem.* **2010**, *82*, 9028−9033.
(28) Riccardi, C. D.; Yamanaka, H.; Josowicz, M.; Kowalik, J.; Mizaikoff, B.; Kranz, C. *Anal. Chem.* **2006**, *78*, 1139−1145.
(29) Lassalle, N.; Mailley, P.; Vieil, E.; Livache, T.; Roget, A.; Correia, J. P.; Abrantes, L. M. *J. Electroanal. Chem.* **2001**, *509*, 48−57.
(30) Nie, G.; Bai, Z.; Chen, J.; Yu, W. *ACS Macro Lett.* **2012**, *1*, 1304−1307.
(31) Corrigan, D. K.; Schulze, H.; McDermott, R. A.; Schmuser, I.; Henihan, G.; Henry, J. B.; Bachmann, T. T.; Mount, A. R. *J. Electroanal. Chem.* **2014**, *732*, 25−29.
(32) Malhotra, B. D.; Kumar, N.; Chandra, S. *Prog. Polym. Sci.* **1986**, *12*, 179−218.
(33) Spires, J. B.; Peng, H.; Williams, D.; Travas-Sejdic, J. *J. Electroanal. Chem.* **2011**, *658*, 1−9.
(34) Spires, J. B.; Peng, H.; Williams, D. E.; Soeller, C.; Travas-Sejdic, J. *Electrochim. Acta* **2010**, *55*, 3061−3067.
(35) Serra Moreno, J.; Panero, S. *Electrochim. Acta* **2012**, *68*, 1−8.
(36) Braslavsky, I.; Hebert, B.; Kartalov, E.; Quake, S. R. *Proc. Natl. Acad. Sci. U.S.A.* **2003**, *100*, 3960−3964.
(37) Palanisamy, R.; Connolly, A. R.; Trau, M. *Bioconjugate Chem.* **2010**, *21*, 690−695.
(38) Ball, R.; Blunt, M. *J. Phys. A: Math. Gen.* **1988**, *21*, 197.
(39) Lawrence, H.; Taylor, G.; Millar, C.; Lambert, D. *Conserv. Genet.* **2008**, *9*, 1293−1301.
(40) Sambrook, J., Fritsch, E. F., Maniatis, T. *Molecular Cloning: A Laboratory Manual*; Cold Spring Harbor Laboratory Press: Cold Spring Harbor, NY, 1989.

DOI: 10.1021/acs.analchem.5b00079
Anal. Chem. XXXX, XXX, XXX−XXX